J. agric. Engng Res. (1997) **68,** 291–296

Simple, Low-Cost Image Analysis of Soil Pore Structure

E. A. G. Robertson; D. J. Campbell

Soils Department, SAC, Bush Estate, Penicuik, Midlothian EH26 0PH, UK

(Received 28 February 1996; accepted in revised form 14 August 1997)

A low-cost method to obtain and analyse digital images of prepared soil sample faces is described. Soil samples are stabilized and pore space is highlighted using a hard-setting resin. The sample faces are photographed using a 35 mm SLR camera fitted with a macro-lens and digital images of the negatives or slides are transferred on to Kodak Photo-CD. The images are analysed using custom-written software on a standard IBM-compatible PC. Various soil structural characteristics are evaluated that have previously required greater resources for evaluation.

The method is illustrated with images of three contrasting soil compaction treatments from a field experiment and the results obtained are examined in relation to gas movement measurements.

1. Introduction

In order to characterize the structural organization within a soil sample, it was decided to investigate the use of simple image analysis techniques on soil core samples. It was considered that image analysis applied to various surfaces cut through a soil core would provide a more complete picture of soil structure as it varies within a sample. Measurements of air permeability and gas diffusion are commonly used to provide information on the structural state of intact soil samples collected from field sites, and can also be of use with remoulded samples in laboratory studies.[1]

A limitation of gas movement measurement techniques is that they are carried out on a whole-sample basis, with no information about the spatial variation and effect of individual pores or pore sizes within the sample. As minimally disturbed cores obtained from field sites may often contain quite distinct layers, the most restricting layer will determine the result. It was considered appropriate to try to combine the gas transport measurements with some more detailed information about the pore structure that produced them.

In the past, image analysis has tended to involve the use of expensive, dedicated equipment. Moran *et al.*[2] and McBratney and Moran[3] provided a reasonably straightforward procedure for preparing and analysing images of soil. Unfortunately, the resin used by Moran *et al.*[2] to stabilize samples and highlight pore space is not readily available in the UK and they used an expensive workstation to analyse the images. Vermeul *et al.*[4] used a high-contrast photographic processing technique to obtain prints that were digitized using a desktop scanner. This approach removes any opportunity to obtain wider information from the original image. The method of heating the sample to allow the impregnation of the wax marker meant that all of the connected macroporosity within the sample could be filled with wax.

This paper describes a simple, low-cost procedure for preparing samples and obtaining and analysing images based on locally available products and services and a PC-style computer. The resin used does not mix with water so that it marks pore space involved in gas transport only. The storage of the images in colour on Photo-CD offers the opportunity to analyse the images using more rigorous methods, should the facilities become available.

2. Materials and method

In this study, image analysis involves a series of operations to obtain and analyse a digital image, representative of soil structure. The work was carried out on minimally disturbed cores taken from a field experiment. The field experiment was sited on Macmerry series soil and comprised four blocks of five randomly positioned treatments. Three of the treatments in the first two of the blocks were sampled, namely zero traffic (ZT), light traffic (LT) and heavy traffic (HT). The LT treatment was provided by running a concrete roller on the plots after cultivation and again after drilling. The HT treatment was applied using a case 1394 (two-wheel drive) tractor which was loaded with front weights and a tractor-mounted Kuhn rotovator. ZT received no traffic after sowing. The three treatment areas were previously ploughed, rotovated and sown with winter barley, and all three were subsequently rolled with a cambridge roller.

Samples were obtained one week after sowing, after the barley had germinated but before this was visible on the soil surface. The core samples are 50 mm deep with an inside diameter of 73 mm. The steel sampling cylinders have a sharpened cutting edge and are hammered into the soil at the selected depth. In this case the uppermost 10 mm of soil was removed to provide a level surface, resulting in core samples from 10 to 60 mm. When the sample ring has been dug out of the soil, the open sample faces are trimmed to give a sample of approximately 209 cm^3. The relative diffusivity and air permeability of each core sample was measured[1] at field water content.

The following steps are required to obtain digital images from the core samples. First, a resin is added which sets hard and serves to stabilize the soil core sample and highlight structural features. The polyester resin is a readily available and reasonably inexpensive product called "Fastglas" (W. David & Sons Ltd., Wellingborough, Northants, England, NN8 2QP); it is supplied as a thick liquid resin and a tube of hardener which must be combined to set. Acetone is used as a diluent in the resin and "Oracet yellow 8GF" dye (Ciba-Geigy Pigments, Clayton, Manchester, England, M11 4AR) is also mixed into the resin. A combination of 50 ml resin, 15 ml acetone, 20 cm hardener and 0·5 g of dye is thoroughly mixed and applied to the upper surface of the samples. The dilute resin has a low viscosity and this allows the resin to travel into the pore space within the sample. Adhesive tape is used to form a collar around the target surface of the sample. The resin mix is trickled onto the surface and finds its way into the pores. It is best to avoid ponding the sample surface as the resin sets more rapidly in the absence of air. A second, less dilute, application is required to fill up larger pore spaces such as worm channels. The dye provides good contrast between the soil particles and the resin-filled pores. This contrast is greatly enhanced under ultraviolet illumination as the yellow dye fluoresces.

The sample can then be cut open at the desired horizontal or vertical plane. The exposed face is then photographed using an ordinary 35 mm SLR camera fitted with a macro-lens which allows close-up focusing so that the frame of the film can be filled with the subject. As a safe alternative to UV light, a long-wavelength fluorescent tube light was used to illuminate the sample. However, this produced a blue light which caused a distinct blue cast in photographs so a Cibachrome 0·5 yellow filter and a UV filter were placed over the lens to correct the colour cast and to block near UV light which can adversely affect photographic film.

Table 1
Image resolution in pixels and size of the 8-bit grey-scale file obtained using the Kodak Photo-CD system. The five versions of each image are stored as one compressed file on the CD

Length, pixels	*Width, pixels*	*File size, bytes*
128	192	25 630
256	384	99 358
512	768	394 270
1024	1536	1 573 918
2048	3072	6 292 510

The next step was to digitize the photographs, i.e. to convert the image in the photograph into a computer-readable form. In this study, Kodak's Photo-CD transfer service was used. This is a service whereby 35 mm monochrome or colour, negatives or slides are scanned at five resolutions and stored on a compact disc. Such compact discs can be accessed on a PC equipped with a compatible CD-ROM drive and some appropriate software. Unfortunately, the transfer service is not immediate and so it is very important to ensure that enough suitable photographic images are obtained in the first instance. Alternatively, samples should be retained to allow further photographs to be obtained. Although each image is stored as a 24-bit colour file at the five resolutions noted in Table 1, a simpler 8-bit grey-scale version of the file was used to simplify the analysis.

Once a digital version of the image is obtained it is a common practice to carry out some pre-processing to ensure that the features of interest are easily identified and quantified.[5] However, as the effects of pre-processing are difficult to gauge on images which contain uncertain and highly varied features, this was limited to segmentation of the images.

The segmentation of an image is the process whereby each pixel of the image is regarded as being a member of any one of two or more sets. In the simple case here, it would be whether the pixel belonged to light-coloured resin-filled pore space or dark-coloured soil solid. In order to segment an image, a threshold value must be selected. The individual pixels are then classified in relation to the threshold value. Selection of the threshold value is subjective in this case. A histogram of the grey-scales is displayed; this usually takes the form of one large peak with a tail to the right. The large peak is generally the larger number of solid soil pixels, while the tail of the peak represents the resin-filled areas.

After the image has been segmented into pore and solid categories, the image is analysed using the methods outlined by McBratney and Moran[3] to provide measures of porosity, pore surface area per unit volume, horizontal pore-star length and horizontal solid-star length. Each of these characteristics is obtained for each horizontal scan-line of the image. The advantage of analysing images in the manner described by McBratney and Moran[3] is that only two horizontal scan-lines, or rasters, of the image are required to be accessed by the analysis program at any one time. This method cannot therefore provide information about the individual pores within an image directly. In order to obtain measurements of individual pores, the locations of the start and end points of pore pixel occurrences on each scan-line are saved to a file during the above analysis.

The resulting file is then imported into Microsoft Excel 5 where a macro is used to re-connect the strings of pore pixels and derive various characteristic factors. Pore-size distribution for the example images are included, while other derived boundary and shape factors require further investigation. The methods noted above allow the use of large high-resolution images containing many pore features to be analysed while avoiding the difficulties in directly managing extended or expanded PC memory.

3. Results

Figure 1 contains typical examples of binary images from cylindrical soil cores from each of three treatments in a field experiment involving various traffic regimes. The area of each sample is 770 pixels deep by 1200 pixels wide. Each sample is approximately 32·6 mm deep by 50·8 mm wide and each pixel is equivalent to an area of 42·3 μm square. *Figure 1(a)* is an image from a zero-traffic treatment (ZT) and it can be seen that the resin has travelled throughout the soil core with only a few areas not reached. *Figure 1(b)* is from a lightly compacted treatment (LT) and the resin is seen to have reached much less of the core with some areas exhibiting no penetrable pore space. *Figure 1(c)* is from a heavily compacted treatment (HT) and shows little penetrable pore space below the uppermost part of the sample. There are very few of the finer pores exhibited by the ZT and LT treatments and this is likely to be caused by the finer pores being less well connected or more likely to contain enough water to stop the progress of the resin.

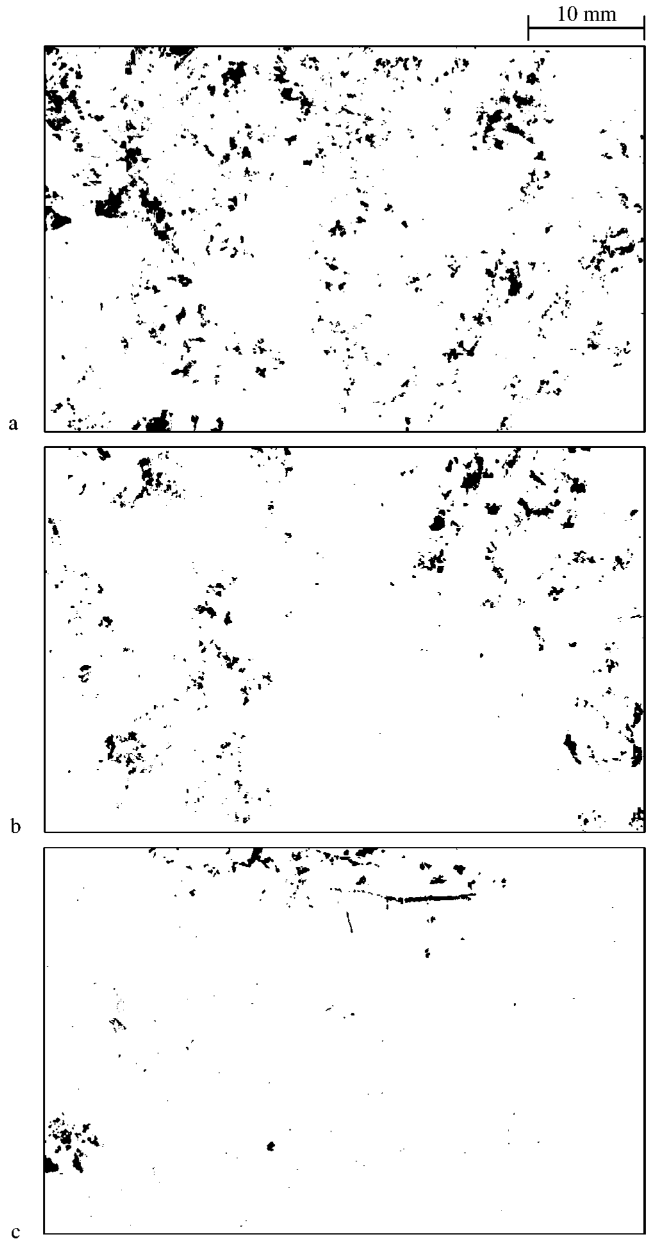

Fig. 1. Binary images from three traffic treatments. Black areas represent pores. (a) zero traffic (ZT); (b) light compaction (LT); (c) heavy compaction (HT). Each image is a vertical face covering a region approximately 15–47 mm depth below the original soil surface

The results of analysing these images are shown in *Figs 2–6*, with the results for one property, shown in each. *Figure 2* shows a graph of the porosity in each scan-line of each of the images, as a volume percentage. This represents the inter-connected, air-filled porosity in each of the three treatments. *Figure 3* is a graph of the soil pore surface area per unit volume and would be of particular interest in studies concerned with gas exchange. *Figures 4* and *5* are graphs of pore horizontal star length and solid horizontal star length, respectively, and these represent the expected continuous length of pore and solid areas in either direction from any random point on each scan-line. The poroid size distributions are obtained from the re-connection procedure and are shown in *Fig. 6* for the three traffic treatments. There are a small number of relatively large pores present, particularly in the ZT image. The number and size of poroids ranks in the expected order with the HT treatment

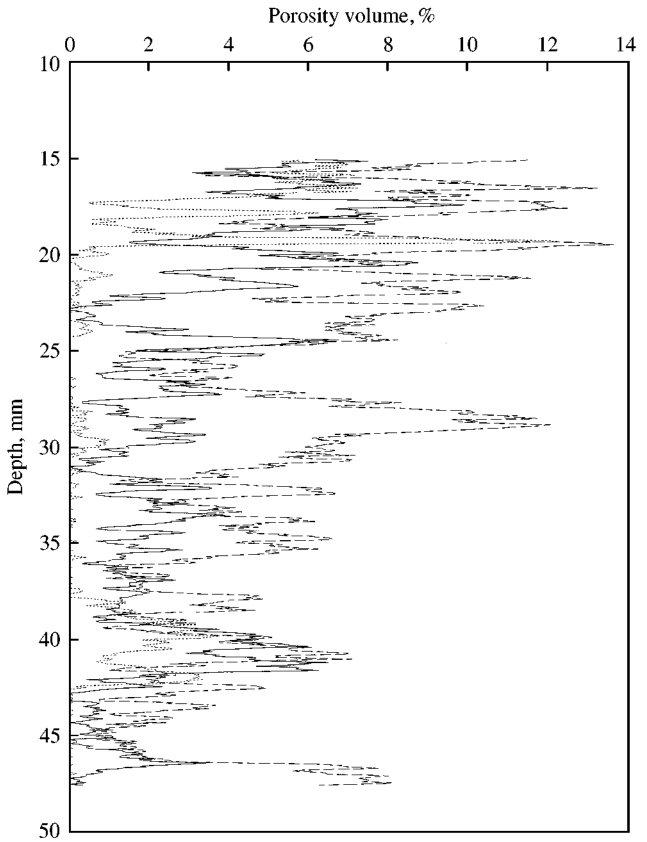

Fig. 2. Porosity shown as a percentage of volume; - - - ZT; —— LT; ········ HT

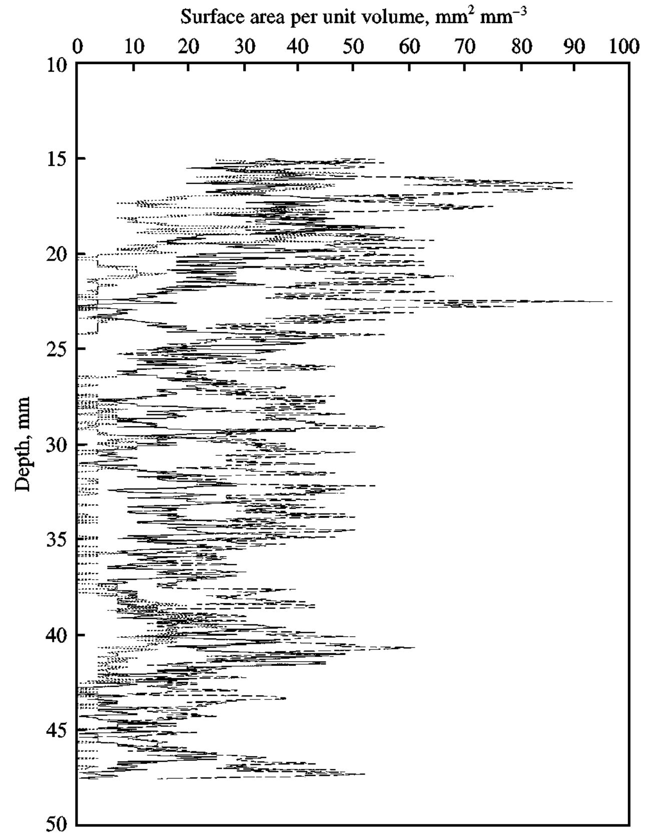

Fig. 3. Surface area of pore space per unit volume; - - - ZT; —— LT; ········ HT

containing fewer and smaller poroids than LT and ZT, respectively.

The images in *Fig. 1* were obtained from core samples that had previously undergone non-destructive gas diffusion and air permeability measurements. The results of the gas movement measurements and other associated data are shown in Table 2. Air permeability had to be log-transformed to give a normal distribution. The standard error (SE) of the log-transformed data was 0·318. The images in *Fig. 1* were selected as typical for each treatment and the results shown in *Figs 2–5* are the results obtained by analysing those images. The data shown in Table 2 are means of four samples for each of two replicate blocks of the three treatments.

4. Discussion

The treatment effect on soil porosity is clearly evident in the binary images in *Fig. 1*. The amount and distribution of porosity within each treatment varies in line with other related soil properties indicated in Table 2. ZT air permeability and gas diffusivity measurements are about twice those for LT, and many times that of HT.

While the gas movement measurements are very sensitive to the compaction treatment, it is likely that values for looser samples such as ZT are exaggerated by gas movement at the sample/sample holder face. This was highlighted by resin that had travelled down the outside of some of the soil samples during preparation. This effect is likely to depend particularly on how coarsely structured the test soil is. It should also be remembered that the faces shown in *Fig. 1* are typical of the faces obtained, and that the pore structure may vary even within the cores that were used to produce *Fig. 1*.

The fact that the total porosities for the three treatments are similar suggests that the differences in gas movement are strongly influenced by the varying ratio of air to water-filled pore space. The images in *Fig. 1* reinforce the premise that water-filled pore space restricts the transport of gas and also highlight structural differences that cause these effects.

The various characteristics in Table 2 are ranked in the order that would appear appropriate from the images of the three treatments in *Fig. 1*. The ZT treatment exhibits lower dry-bulk density and volumetric water content and higher total- and air-filled porosity, air permeability and relative diffusivity. The two compaction

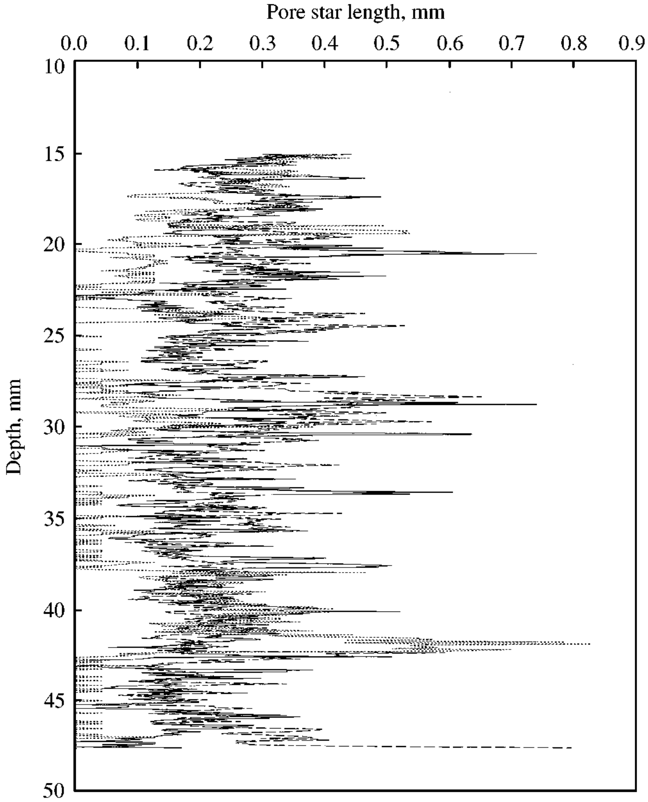

Fig. 4. Horizontal pore star length, mm; --- ZT; —— LT; ········ HT

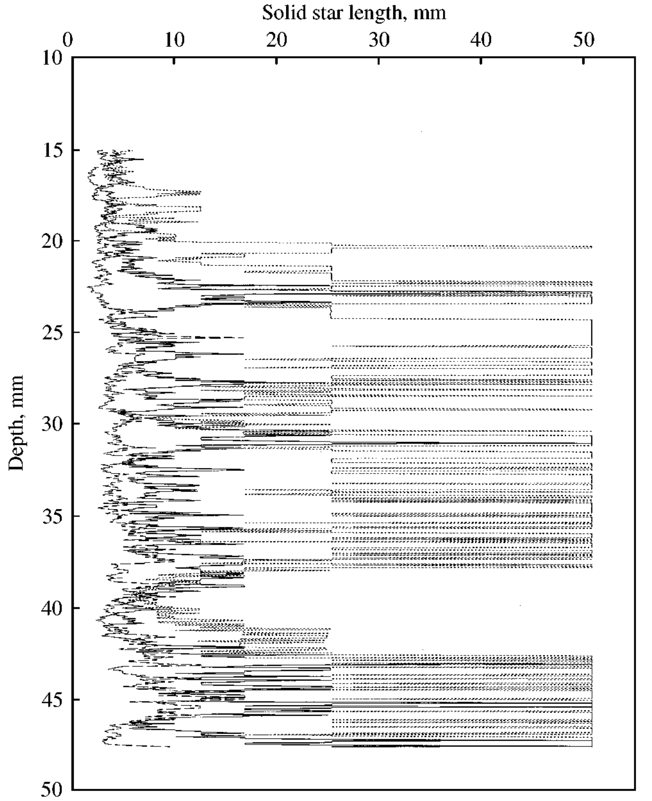

Fig. 5. Horizontal solid star length, mm; --- ZT; —— LT; ········ HT

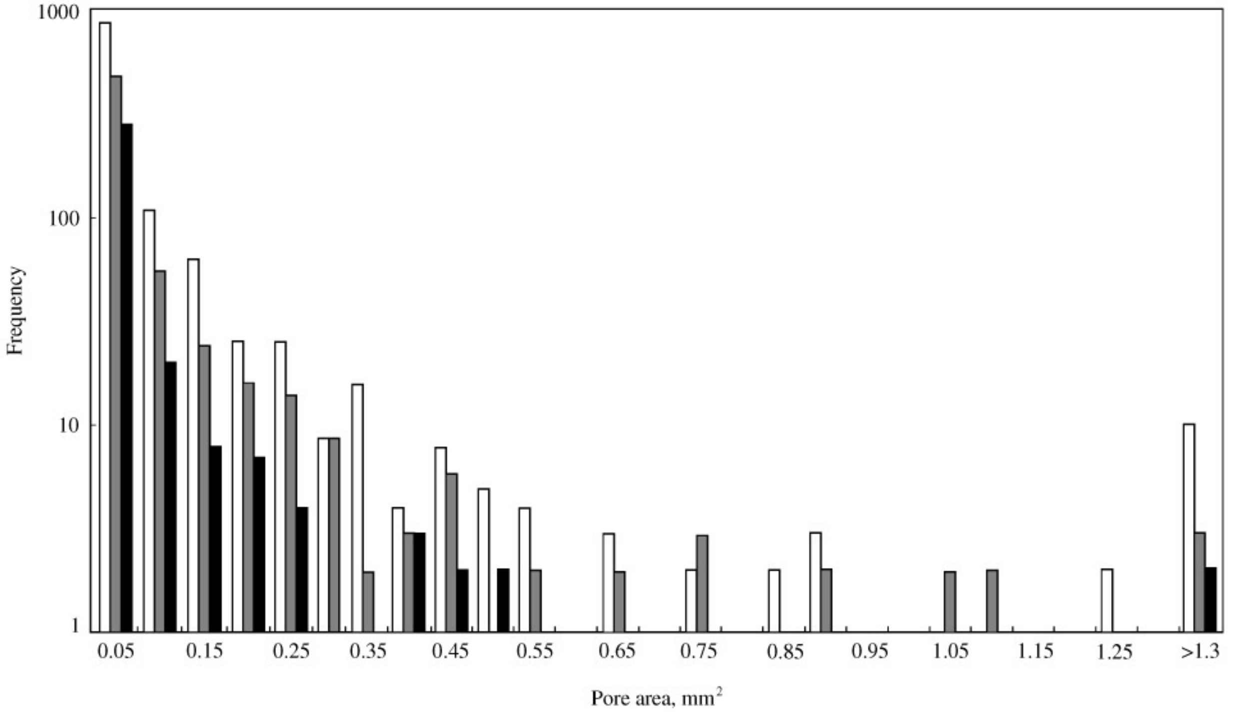

Fig. 6. Pore size distribution; □ ZT; ■ LT; ■ HT

Table 2
Summary of soil core sample information

Treatment	*Dry bulk density, Mg/m^3*	*Water content, by volume*	*Total porosity, m^3/m^3*	*Air-filled porosity, m^3/m^3*	*Air permeability, μm^2*	*Relative diffusivity*
ZT	1·047	0·299	0·597	0·299	924·0	0·069719
LT	1·142	0·325	0·561	0·236	523·4	0·031842
HT	1·264	0·395	0·514	0·119	2·3	0·000838
SE	0·030	0·018	0·012	0·029	—	0·008

treatments have higher dry-bulk density and volumetric water content and lower porosity, permeability and diffusivity.

The pore characteristics shown in *Figs 2–6* are consistent with the qualitative treatment effects displayed in *Fig. 1. Figure 3* provides an indication of the surface area of the pores and it shows that the pores in ZT provide a greater surface for gas exchange or other chemical or biological activities than either of the two compaction treatments.

Figure 4 describes the variation in horizontal pore star length down the samples faces. Pore star length does not directly represent pore size. It provides an indication of how this varies with depth and between treatments. The HT treatment contains many scan-lines with only one or with no pixels at all marked as pore space. Similarly, *Fig. 5* shows that, in many cases, the individual scan-lines of the HT image consist of solid soil as denoted by the solid horizontal star length being equal to the sample width. Both ZT and LT exhibit a variable pore horizontal star length (*Fig. 4*) throughout the samples, while *Fig. 5* shows a steadily increasing solid star length for the LT treatment. This suggests that the pores present in the ZT treatment are smaller at depth, while the pores present in the LT treatment vary less in size but are positioned closer together at depth. The small but distinct increase in solid star length (*Fig. 5*) in the ZT treatment at about 31 mm depth may emphasize the position of a restrictive layer within that sample.

It should be noted that *Figs 1–6* describe the variation in specific properties observed on two-dimensional faces and as such can only provide information on how the properties vary across the chosen sample face.

5. Conclusions

The automated analysis of sample images helps to provide information on how structural features control gas movement while providing numerical information that may be used in statistical analysis.

The new method represents a relatively simple introduction to sample preparation and the transfer of photographs to Photo-CD is an effective method for obtaining digital images. The minimal start-up costs and the likelihood that many laboratories may already possess much of the necessary equipment, means that the method could be useful in a wider range of situations where preliminary or low-volume image processing and analysis is required.

Acknowledgement

The authors would like to thank J. K. Henshall for providing an image manipulation program to which the image analysis routines were attached and the reconnection macro. Dr B. C. Ball provided access to a field experiment for sampling purposes.

We acknowledge the financial support of the Scottish Office Agricultural Environment and Fisheries Department.

References

[1] **Ball B C; Harris W; Burford J R** A laboratory method to measure gas diffusion and flow in soil and other porous materials. Journal of Soil Science, 1981, **32,** 323–333

[2] **Moran C J; McBratney A B; Koppi A J** A rapid method of analysis for soil macropore structure: I. Specimen preparation and digital binary production. Soil Science Society of America Journal, 1989, **53,** 921–928

[3] **McBratney A B; Moran C J** A rapid method of analysis for soil macropore structure: II. Stereological model, statistical analysis, and interpretation. Soil Science Society of America Journal, 1990, **54,** 509–515

[4] **Vermeul V R; Istok J D; Flint A L; Pikul, Jr J L** An improved method for quantifying soil macroporosity. Soil Science Society of America Journal, 1993, **57,** 809–816

[5] **Glasbey C A; Horgen G W** Image Analysis for the Biological Sciences, 218 Pp. Chichester, England: Wiley, 1995